Journal of Macromolecular Science, Part A
Publication details, including instructions for authors and subscription information:
http://www.informaworld.com/smpp/title~content=t713597274

Synthesis of Reactive Organifier for the Epoxy/layered Silicate Nanocomposite and the Properties of the Epoxy Nanocomposites

Sang Ki Chung[a]; Jeong Jae Wie[b]; Byeong Yeol Park[a]; Sung Chul Kim[b]
[a] Agency for Defense Development, The 1st R&D Institute-6, Daejeon, Korea [b] Department of Chemical and Biomolecular Engineering, Korea Advanced Institute of Science and Technology, Yuseong-gu, Daejeon, Korea

To cite this Article Chung, Sang Ki , Wie, Jeong Jae , Park, Byeong Yeol and Kim, Sung Chul(2009) 'Synthesis of Reactive Organifier for the Epoxy/layered Silicate Nanocomposite and the Properties of the Epoxy Nanocomposites', Journal of Macromolecular Science, Part A, 46: 2, 205 — 214

To link to this Article: DOI: 10.1080/10601320802595185

URL: http://dx.doi.org/10.1080/10601320802595185

Journal of Macromolecular Science®, *Part A: Pure and Applied Chemistry* (2009) **46**, 205–214

ISSN: 1060-1325 print / 1520-5738 online
DOI: 10.1080/10601320802595185

Synthesis of Reactive Organifier for the Epoxy/layered Silicate Nanocomposite and the Properties of the Epoxy Nanocomposites

SANG KI CHUNG[1], JEONG JAE WIE[2], BYEONG YEOL PARK[1] and SUNG CHUL KIM[2,*]

[1]*The 1st R&D Institute-6, Agency for Defense Development, Yuseong P.O. Box 35, Daejeon 305-600, Korea*
[2]*Department of Chemical and Biomolecular Engineering, Korea Advanced Institute of Science and Technology, 373-1 Guseong-dong, Yuseong-gu, Daejeon 305-701, Korea*

Received July 2008. Accepted August 2008

Reactive organifiers with hydroxyl end-group or amine end-group and with relatively high molecular weight were synthesized. The d-spacing of the organoclays prepared varied from 1.37 nm to 1.98 nm. To disperse nanoparticles into the epoxy matrix resin more efficiently, the sonication cavitation technique was applied. The epoxy/layered silicate nanocomposites were fabricated by *in situ* polymerization using the autoclave curing process. The epoxy resin was based on diglycidyl ether of bisphenol-A (DGEBA type) and diaminodiphenylsulfone (DDS). The epoxy/layered silicate nanocomposites formed exfoliated and intercalated structure with some disorder. The thermal stability, tensile properties, fracture toughness were significantly increased with increasing the dispersibility of the organoclay. The critical stress intensity factor(K_{IC}) of 3wt% OC J230 (organoclay with reactive amine end group) was 2.78 times higher than that of the neat epoxy specimen.

Keywords: Organifier, organoclay, epoxy/layered silicate nanocomposite

1 Introduction

Epoxy resin has been widely used as one of the most important matrix for the composite materials. Although epoxy exhibits good mechanical properties, epoxy has some disadvantages, for example, low fracture toughness and brittleness due to the relatively high crosslink density. To improve the fracture toughness of the epoxy resin, the incorporation of the layered silicate has been extensively studied (1–7). The reason for this trial is that the reactants of the epoxy resin possess suitable polarity in order to diffuse into the clay layer and to form delaminated nanocomposite during polymerization (8). One of the most important phenomena is the self-polymerization of epoxy resin in organophilic smectite clays due to the presence of the alkylammonium ions (1). Park et al. (9) summarized the results to date on epoxy-clay nanocomposite system.

In this study, reactive organifiers which have tertiary amine group in the backbone based on MDEA(N-methyl diethanol amine) and reactive hydroxyl or amine end-group to react with epoxy group during polymerization were synthesized. The epoxy/layered silicate nanocomposites were synthesized by *in situ* polymerization using these organifiers, with controlling the dispersibility of organoclay in epoxy matrix. The effect of the dispersibility of the organoclay on the properties of the epoxy/layered silicate nanocomposites such as the morphology, thermal stability, tensile properties and fracture toughness were investigated.

2 Experimental

2.1 Materials

N-methyl diethanol amine (MDEA, ATOFINA Co., Inc., USA, 99%), poly(tetra methylene glycol) (PTMG, Mn = 2,000, Aldrich Chemical Co., Inc., USA), Jeffamine D400(polyoxypropylenediamine, Huntsman, USA) and Jeffamine D230(Huntsman, polyoxypropylenediamine, USA) were degassed overnight at 70–80°C under vacuum to remove moisture before use. Hexamethylene diisocyanate (HDI, Tokyo Kasei Kogyo Co., Ltd., Japan, 98%) and di-n-butyltin dilaurate (T-12, Tokyo Kasei Kogyo Co., Ltd., Japan) were used without further purification. Diglycidyl ether of Bisphenol-A (DGEBA) type epoxy resin

---

*Address correspondence to: Sung Chul Kim, Department of Chemical and Biomolecular Engineering, Korea Advanced Institute of Science and Technology, 373-1 Guseong-dong, Yuseong-gu, Daejeon 305-701, Korea. E-mail: kimsc@kaist.ac.kr

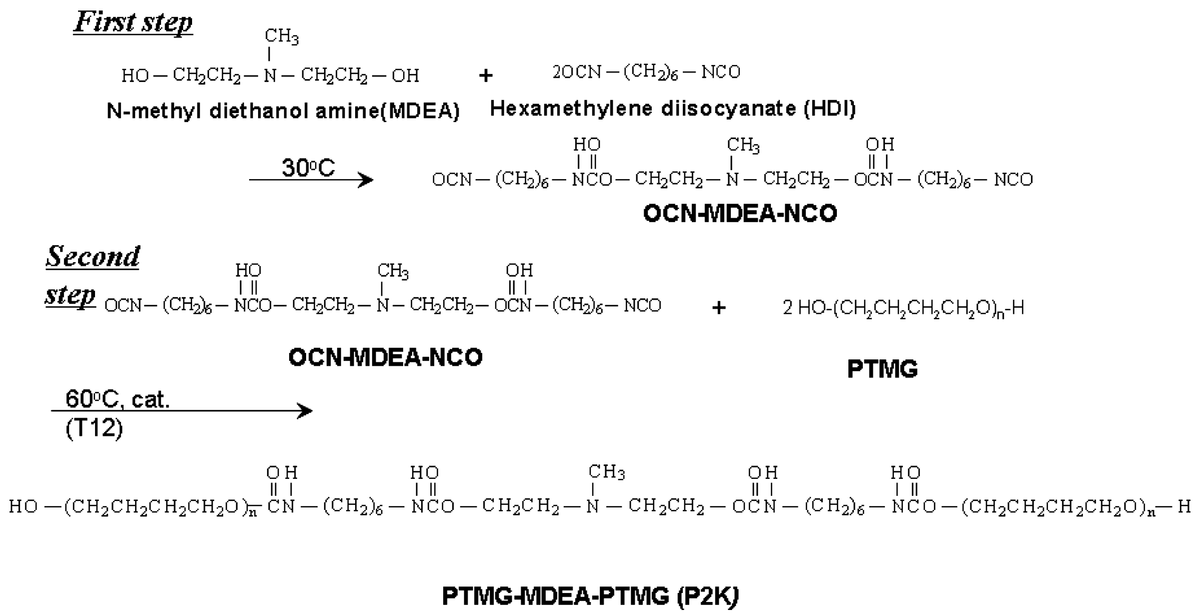

Fig. 1. Reaction scheme for the synthesis of P2K organifier.

(YD128, $M_n = 378$, Kukdo Chemical Co., Korea) was used as a matrix resin and 4,4′-diaminodiphenylsulfone (DDS, $M_n = 248$, Aldrich Co.) was used as a curing agent. The epoxy resin and the curing agent were mixed in 1:1 equivalent ratio. Cloisite® Na^+ (Southern Clay Products, Inc., USA, CEC = 92.6 meq/100 g) was used as the pristine montmorillonite.

2.2 Synthesis of Organifier (10)

The organifier was synthesized by a two-step method as shown in Figures 1 and 2. First, diisocyanate-terminated MDEA (OCN-MDEA-NCO) was prepared by reacting 2 equiv. of HDI with 1 equiv. of MDEA by dropping MDEA in HDI (Figure 1, first step). The reaction was carried out under nitrogen at 30°C until the theoretical isocyanate

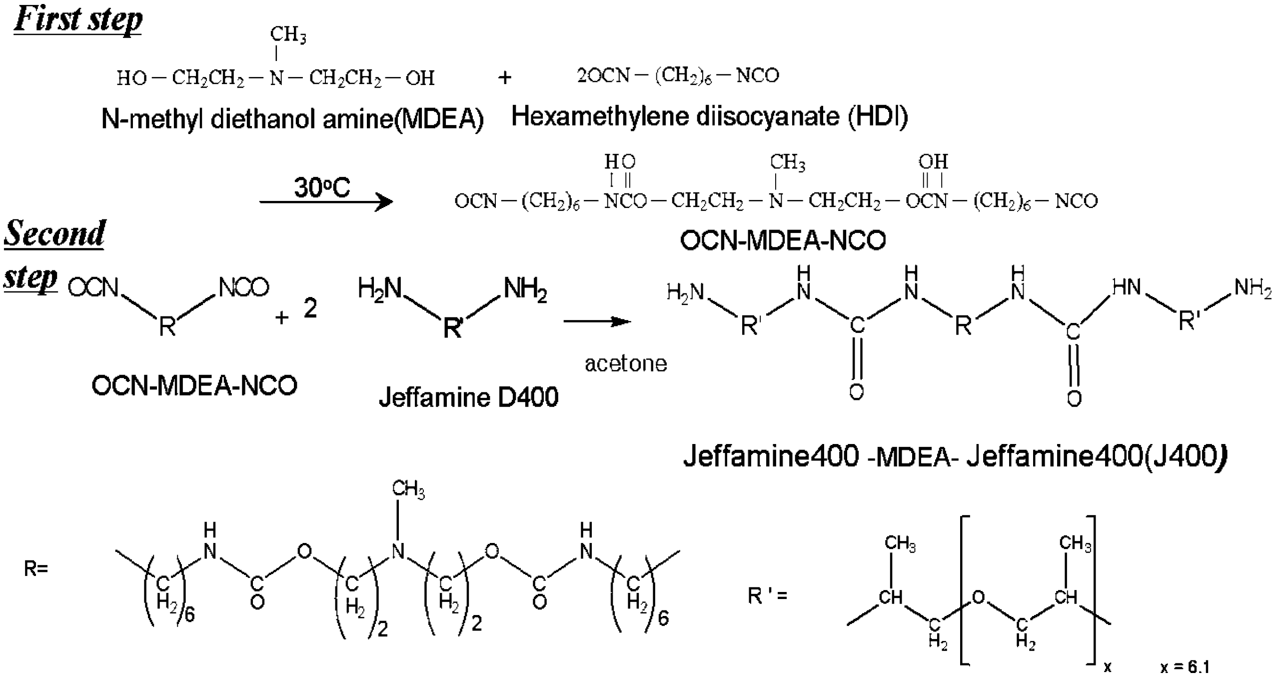

Fig. 2. Reaction scheme for the synthesis of J400 organifier.

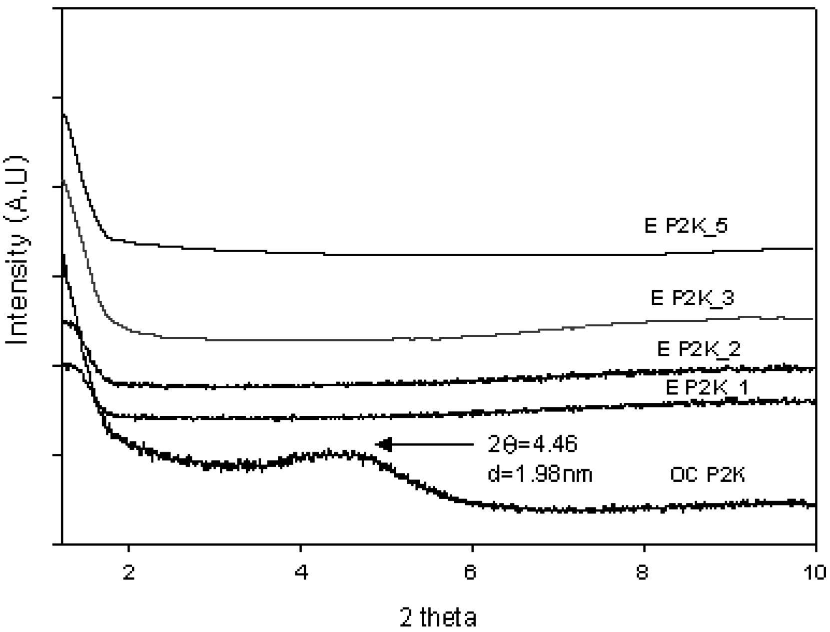

Fig. 3. XRD patterns of E P2K nanocomposites.

content (as determined by the di-n-butylamine titration method (11)) was reached. The hydroxyl terminated organifier was synthesized by reacting 2 equiv. of PTMG with 1 equiv. of OCN-MDEA-NCO (Figure 1, second step) under nitrogen conditions at 60°C. 0.05 wt% of dibutyltin dilaurate (T-12) was added as a catalyst. The amine terminated organifier was synthesized by reacting 2 equiv. of Jeffamine D400 or Jeffamine D230 with 1 equiv. of OCN-MDEA-NCO (second step in Figure 3) under nitrogen conditions at 30°C pouring in acetone. All the reactions were terminated until the peak for the isocyanate group disappeared in the FT-IR measurement.

The notation for the hydroxyl or amine terminated organifier is as follows. PTMG-MDEA-PTMG was coded as P2K, Jeffamine400-MDEA-Jeffamine400 was coded as J400, Jeffamine230-MDEA-Jeffamine230 was coded as J230, respectively. After the cation exchange reaction, the organoclays prepared were named similarly as OC P2K,

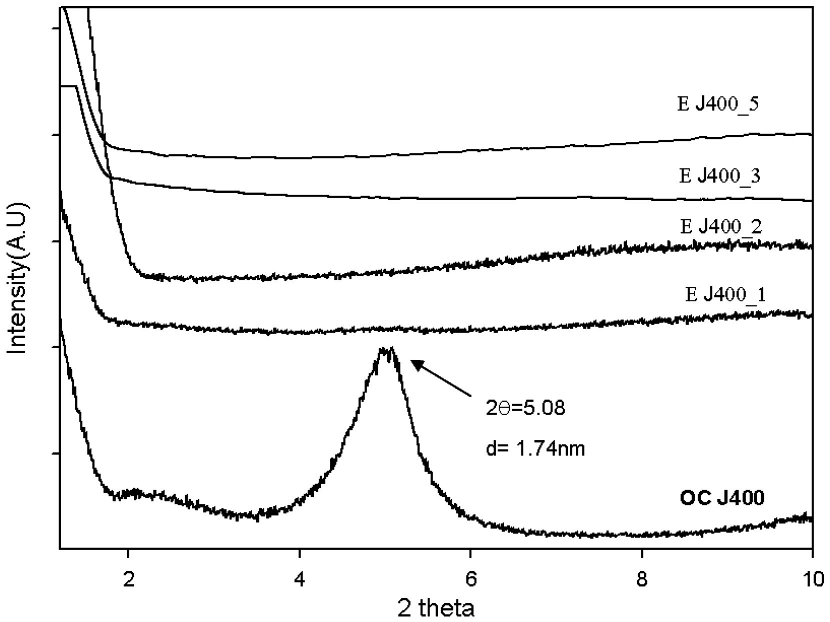

Fig. 4. XRD patterns of E J400 nanocomposites.

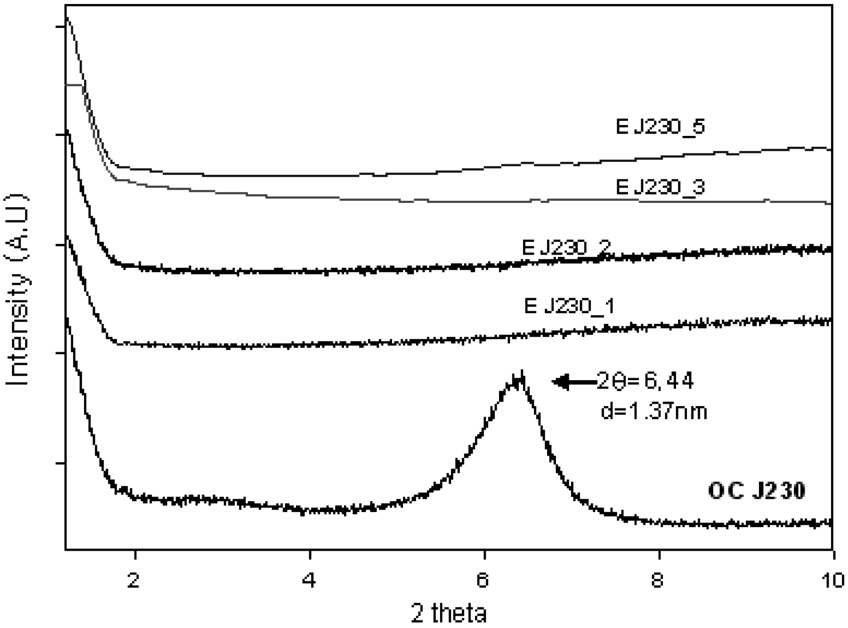

Fig. 5. XRD patterns of E J230 nanocomposites.

OC J400 and OC J230, respectively. The word OC means organoclay.

2.3 Preparation of Organoclay

Organoclays were prepared by cation exchange reaction between the pristine montmorillonite and excess organifier (two times the cation exchange capacity of pristine montmorillonite) (12). The organifier was dissolved in deionized water at 65°C and concentrated HCl was dropped into the organifier solution to quaternize the amine group. The pristine montmorillonite (15 g) was preliminarily dispersed in deionized water (1000 ml) at 65°C by using a mechanical stirrer. Cloisite®Na$^+$ (Southern Clay Products, Inc., USA, CEC = 92.6 meq/100 g) was used as the pristine montmorillonite. The organifier solution was poured into the suspension of the pristine montmorillonite and the mixture was vigorously stirred by using a mechanical stirrer for 24 h at 65°C. The cation-exchanged clay particles were collected by centrifuge and subsequently washed with deionized water until no further formation of AgCl by an $AgNO_3$ test to confirm the absence of halide anions. The organoclays were freeze-dried for 2 days. Dried organoclays were crushed by using a mortar and sieved below 200 μm. The crushed clay was dried at 80°C in a vacuum oven for 1 day. The organoclays in this study were coded as OC P2K, OC J400 and OC J230, respectively.

2.4 Synthesis of Epoxy/Layered Silicate Nanocomposites

Epoxy/Layered silicate nanocomposites were prepared using three kinds of different organoclays (OC P2K, OC J400 and OC J230). The epoxy (DGEBA) resin was mixed with the desired amount of organoclays. To mix better, ultrasonic cavitation technique is used, and it is one of the most efficient means to disperse nanoparticles into a polymer (13–16). Prior to curing, the epoxy resin was mixed with desired amount of clay for 1 h by a sonication method. A stoichiometric amount of the curing agent was added to the DGEBA/organoclay mixture at 140°C with vigorous stirring. The mixture was poured in a fluoropolymer coated aluminum mold and a Teflon mold. All samples were cured for 2 h at 150°C and 2 h at 190°C in an autoclave under 100 psi pressure. A differential scanning calorimeter analysis of the samples confirmed that they were fully cured. The sample code name of epoxy/layered silicate nanocomposites was as follows. E x_y. Where E means epoxy composite, x is the name of the organoclay and y represents wt% of the organoclay.

2.5 Characterization

SEM (Scanning Electron Microscopy) was used to investigate the degree of dispersion of the silicate layers in epoxy matrix. The fractured surface of the nanocomposite was observed by using a Jeol JSM-5610 SEM. TEM specimens were prepared by using a RMC MT-XL microtome with a cryogenic CR-XL system. The specimens were cut with a diamond knife at 25°C. TEM micrographs were obtained by using a Phillips CM20 Transmission Electron Microscopy. Wide-angle X-ray diffraction was obtained at ambient temperature on Rigaku D/MAX-RC diffractometer with CuKα radiation to measure the d-spacing of the organoclays. Each sample was scanned from $2\theta = 1.2°$ to 10° at a scan rate of 2°/min. Thermogravimetric analysis was performed under a nitrogen atmosphere by using a TA

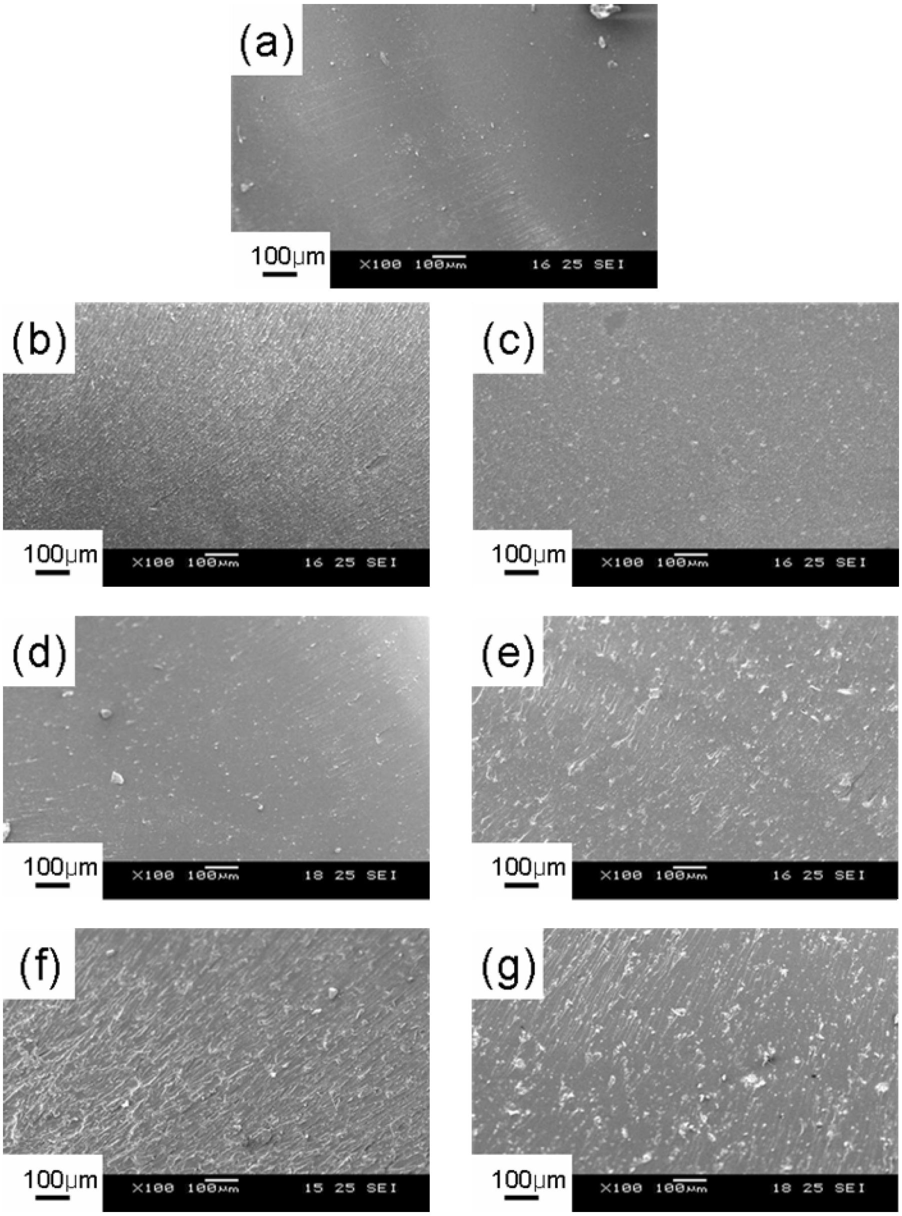

Fig. 6. SEM micrographs of fractured surface of neat epoxy and epoxy/layered silicate nanocomposites (a) neat epoxy; (b) E P2K_1; (c) E P2K_2; (d) E J400_1; (e) E J400_2; (f) E J230_1; (g) E J230_2.

Instruments TGA Q500 to measure the ion exchange fraction of organoclay and the thermal stability of epoxy and epoxy/layered silicate nanocomposites. The measurement was carried out with a heating rate of 20°C/min in the temperature range from 50 to 950°C. The ion-exchange fraction is defined as the fraction of sodium cation exchanged by the organifier by a cation exchange reaction.

2.6 Tensile Properties

Tensile tests were carried out with the Instron 5583 machine according to ASTM D638M. The grip distance of 25 mm was used and the crosshead speed was 50 mm/min.

2.7 Fracture Toughness

The fracture toughness was measured in terms of the critical stress intensity factor(K_{IC}). It was measured using single edge notch bending(SENB, 3-point-bending), by ASTM E399-78a. The dimension of the specimen was 3 × 6 × 60 mm (rectangular bar). Specimens were pre-cracked by inserting a razor blade into the machined notch and impacting with a rubber hammer, crack length was 1.5–3.0 mm, span length was 24 mm, and at least 5 samples were tested. The critical stress intensity factor(K_{IC}) was calculated from the following equation:

$$K_{\mathrm{IC}} = 6P/(BW^{1/2}Y) \tag{1}$$

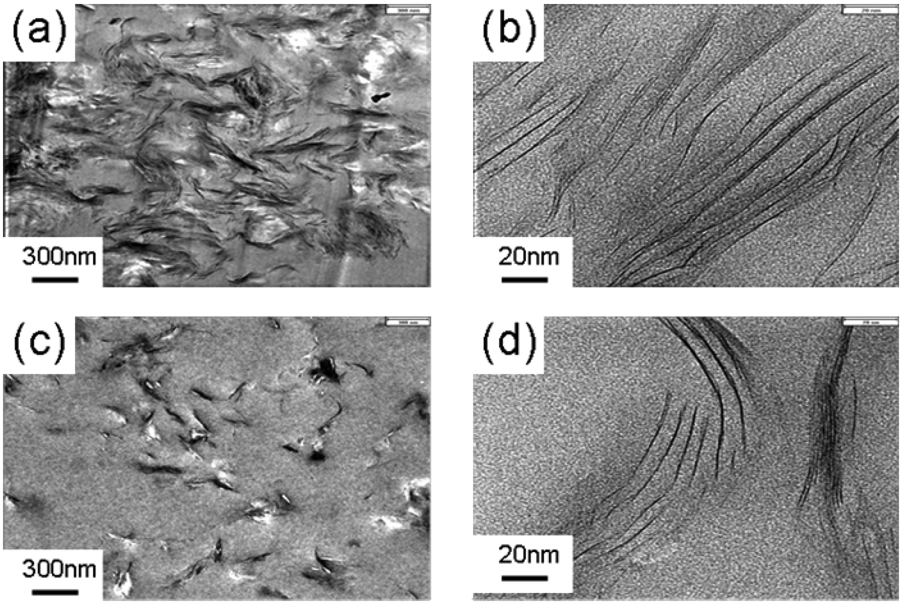

Fig. 7. TEM micrographs of E P2K nanocomposites. E P2K_2 (a) low magnification, (b) high magnification; E P2K_5 (c) low magnification, (d) high magnification.

where P is the applied load, B is width, W is thickness and Y is the sample geometry factor that is defined as:

$$Y = 1.93R^{1/2} - 3.07R^{2/3} + 14.53R^{5/2} \\ -25.11R^{7/2} + 25.80R^{9/2} \qquad (2)$$

where $R = a/W$, and a is the length of the pre-crack.

3 Results and Discussion

3.1 Degree of Dispersion of Organoclay

Reactive organifiers which have tertiary amine group in the backbone based on MDEA(N-methyl diethanol amine) and reactive hydroxyl or amine end-group to react with epoxy group during polymerization were synthesized. In addition, organifiers (organoclays) act as additional curing

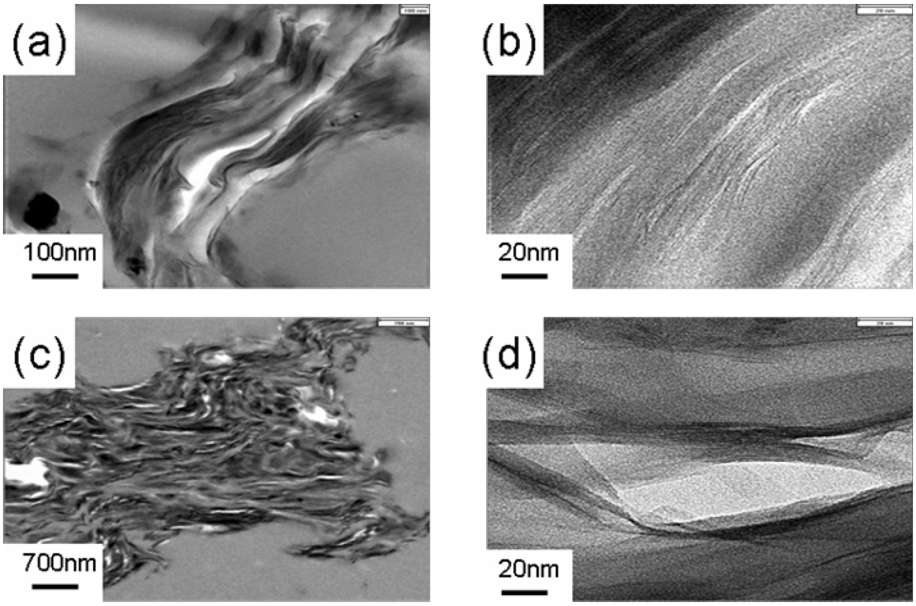

Fig. 8. TEM micrographs of E J400 nanocomposites. E J400_2 (a) low magnification; (b) high magnification; E J400_5; (c) low magnification; (d) high magnification.

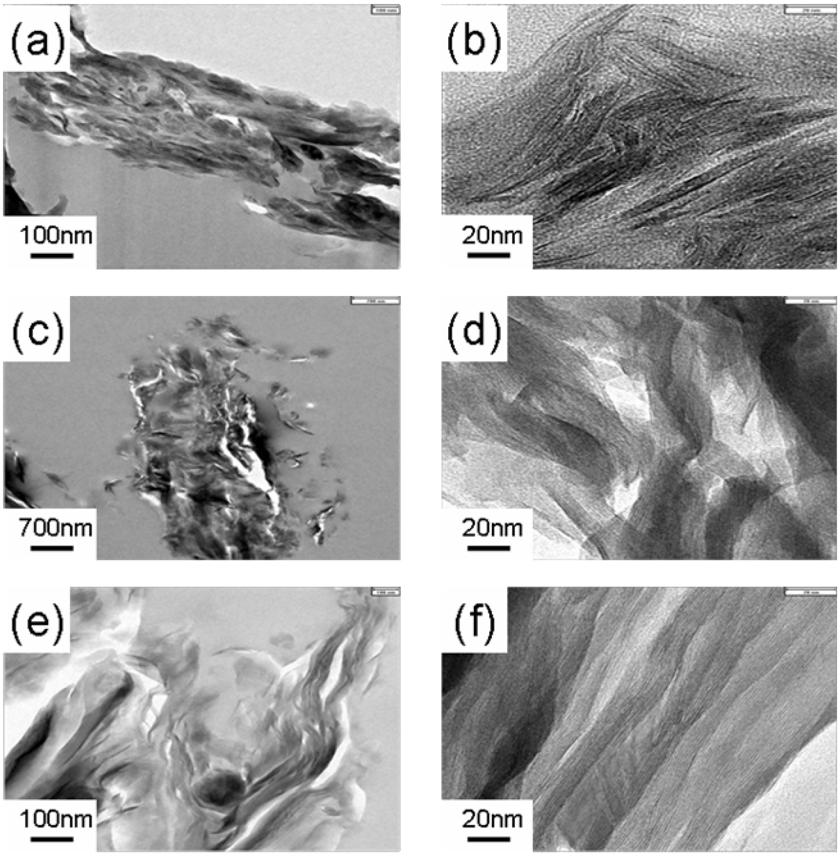

Fig. 9. TEM micrographs of E J230 nanocomposites. E J230_1 (a) low magnification; (b) high magnification; E J230_3; (c) low magnification; (d) high magnification; E J230_5; (e) low magnification; (f) high magnification.

agent. It is reported that during *in situ* polymerization monomers can intercalate into the layered silicate gallery and then polymerize (7). Kornmann also reviewed the phenomenon in *in situ* polymerization that first the organoclay is swollen in the monomer, then the reaction is initiated. For the thermosets such as epoxies or unsaturated polyesters, a curing agent or a peroxide, respectively, is added to initiate the polymerization (8).

Figures 3 to 5 show the XRD patterns for OC P2K, OC J400, OC J230 organoclays and the corresponding epoxy/layered silicate nanocomposites. The d-spacing of pristine montmorillonite is 1.18 nm ($2\theta = 7.48^\circ$) and the d-spacing increased by introducing the organifier from 1.18 nm ($2\theta = 7.48^\circ$) to 1.98 nm ($2\theta = 4.45^\circ$) for OC P2K, 1.74 nm ($2\theta = 5.08^\circ$) for OC J400, and 1.37 nm ($2\theta = 6.44^\circ$) for OC J230, respectively. By the TGA analysis, the inorganic content of OC P2K was 35.1 wt%, that of OC J400 was 72.31 wt%, and that of OC J230 was 80.5 wt%, and the molecular weight of P2K was 4,445 g/mol, that of OC J400 was 1245 g/mol, and that of OC J230 was 905 g/mol, so the ion-exchanged fraction of OC P2K was 0.448, that of OC J400 was 0.332, and that of OC J230 was 0.288, respectively. The epoxy/layered silicate nanocomposites with upwards of 5% organoclay did not show a significant peak to measure the d-spacing E P2K, E J400 and E J230 series in WAXD measurement. In general, the d-spacing of organoclay in polymer nanocomposites depends on the interaction between the polymer matrix and the organoclay (17) and the preparation method of nanocomposites (18). In all nanocomposites, sonication was applied to the organoclay mixture in epoxy resin before mixing with hardener.

SEM micrographs of the fractured surfaces of E P2K, E J400 and E J230 nanocomposites are shown in Figure 6. In Figure 6, the fractured surface of the neat epoxy shows smooth and featureless surface, so there is no obstruction in the path of the crack, which decreases the resistance to crack propagation. But the fractured surface of E P2K, E J400 and E J230 show the existence of crack-pinning morphology, especially E J230_2 shows typical crack pinning pattern by the clay which is reflected in the fracture energy behavior. Therefore we anticipate E J400 and E J230 have better fracture toughness than E P2K nanocomposite.

TEM micrographs of E P2K, E J400 and E J230 nanocomposites are shown in Figures 7–9. The dark lines represent the side view of MMT layers and the grey background represents the polymer matrix. Nanocomposites show dispersed separated organoclays with thickness ranging from 20 nm to 100 nm. E P2K series nanocomposites

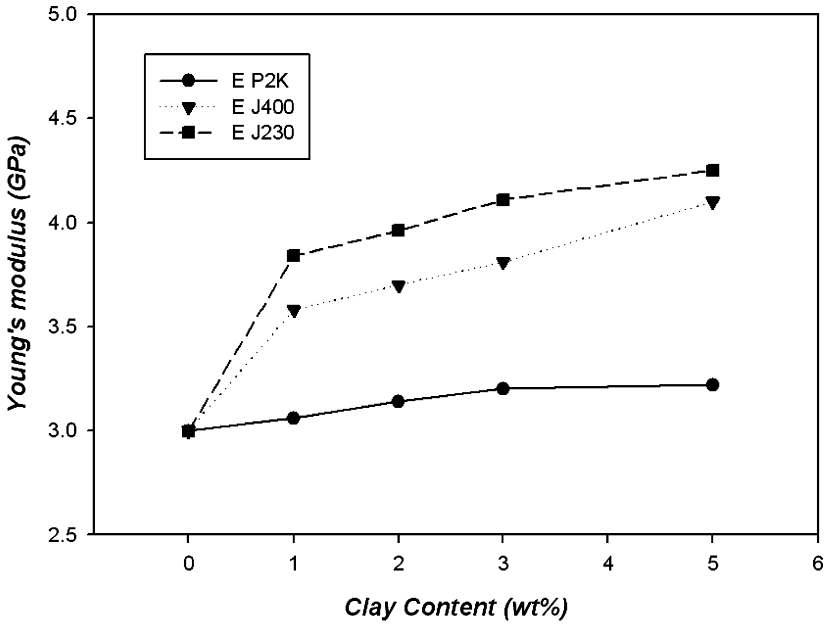

Fig. 10. Young's modulus of epoxy and epoxy/layered silicate nanocomposites.

exhibit relatively better dispersion of the clay and the average distance between the neighboring clay platelet is about 2.9–5.5 nm which is larger when compared to E J400 or E J230 nanocomposites. The E J400_2 formed an ordered intercalated structure, the well-stacked structure of silicate layers is shown in Figure 8. In the case of the E J400 and E J230 nanocomposites, in high magnification, it was found that the intercalated structure with some disorder was formed, but the d-spacing was narrower that the E P2K series nanocomposites. The epoxy/layered silicate nanocomposites formed the intercalated structure with some disorder and their d-spacing was about 0.9–5.5 nm.

3.2 Thermal Stability

The TGA results of the neat epoxy and epoxy/layered silicate nanocomposites are summarized in Table 1. The onset temperature of degradation, the temperature of maximum decomposition rate are denoted as T_{OD} and T_{max}, respectively. In general, layered silicate particles can enhance

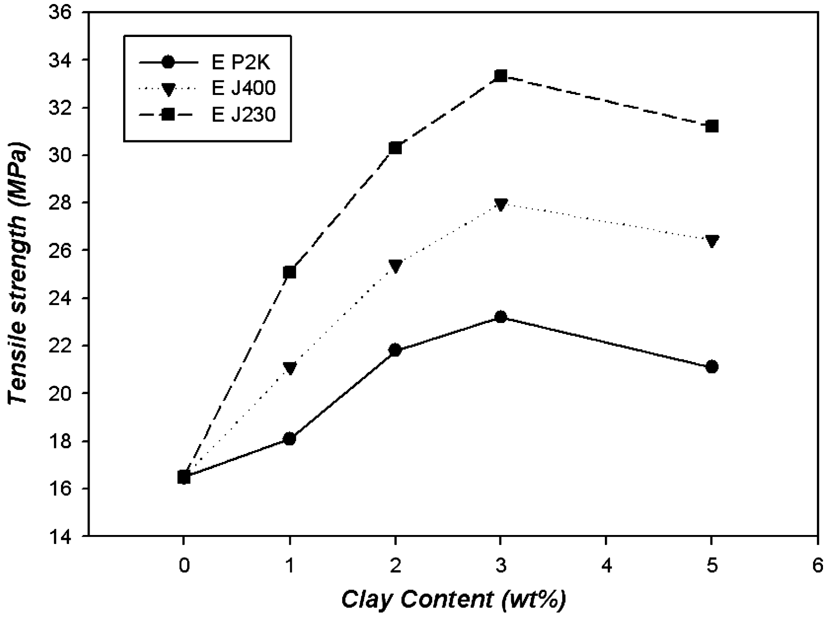

Fig. 11. Tensile strength of epoxy and epoxy/layered silicate nanocomposites.

Table 1. TGA results of epoxy and epoxy/layered silicate nanocomposites.

Sample	*Clay Content (wt%)*	T^a_{OD} (°C)	$T^b_{max,1}$ (°C)
Neat Epoxy	0	418.5	467.3
E P2K_	1	425.1	492.1
	2	424.9	492.2
	3	423.2	482.3
	5	421.0	482.6
E J400_	1	425.3	485.8
	2	423.5	487.8
	3	422.3	482.7
	5	421.3	485.1
E J230_	1	432.0	491.5
	2	420.1	482.5
	3	422.3	480.9
	5	421.3	482.3

[a]T_{OD}: Onset temperature of thermal degradation and [b]$T_{max,1}$: Temperature of maximum decomposition rate for the first degradation stage, respectively

the thermal stability of polymer by acting as mass transport barrier and a heat transfer barrier of the volatile products generated during decomposition (19) and as thermal insulator (20). The effect of clay as thermal and mass transport barrier can be enhanced by improving the degree of dispersion of the organoclay, but no significant difference was observed between E P2K, E J400 and E J 230 although E P2K had the best dispersion of the clay. The T_{max} of epoxy/layered silicate nanocomposites was about 15°C higher than that of neat epoxy due to this clay effect.

3.3 Tensile Properties

The Young's modulus and tensile strength of the neat epoxy and the nanocomposites are shown in Figures 10 and 11. The enhancement of Young's modulus is directly attributed to the reinforcement provided by the dispersed silicate layers (21) and Young's modulus can also be affected by the interfacial interaction between silicate layers and epoxy matrix. There are strong interactions between organoclay and epoxy matrix due to the reaction between organifier and epoxy matrix, so the tensile strength and Young's modulus increased by introducing the organoclay. The Young's modulus (Fig. 10) shows that the modulus increase is significant in E J400 and E J230 nanocomposites. The increase in tensile modulus of the E P2K is not significant due to the well separated silicate layers. In a rigid matrix system like epoxy resin, it seems that the single silicate layer will not provide a significant contribution to the modulus increase. Considering the tensile strength properties, it seems that multi-layer silicate bundles would help the enhancement of the modulus and strength properties. The tensile strength of E J400 and E J230 are significantly higher than that of E P2K. Above 3 wt% of organoclay, however, the tensile strength decreased and we think this is due to the large aggregates formed which act as the defects and stress concentrators in epoxy matrix. E J230 shows the highest modulus and strength increase compared to the other nanocomposites prepared. Modulus increased from 3.0 to 4.2 GPa and tensile strength increased from 16.3 to 33.7 MPa.

3.4 Fracture Properties

The fracture toughness, as quantified by the critical stress intensity factor, K_{IC}, was determined by a three-point bending method. Results of the K_{IC} values are shown in Figure 12. There was dramatic increase in fracture toughness when the clay content was varied from 2 to 3% in all the nanocomposite samples. The K_{IC} of 3 wt% E J230 sample (E J230_3)

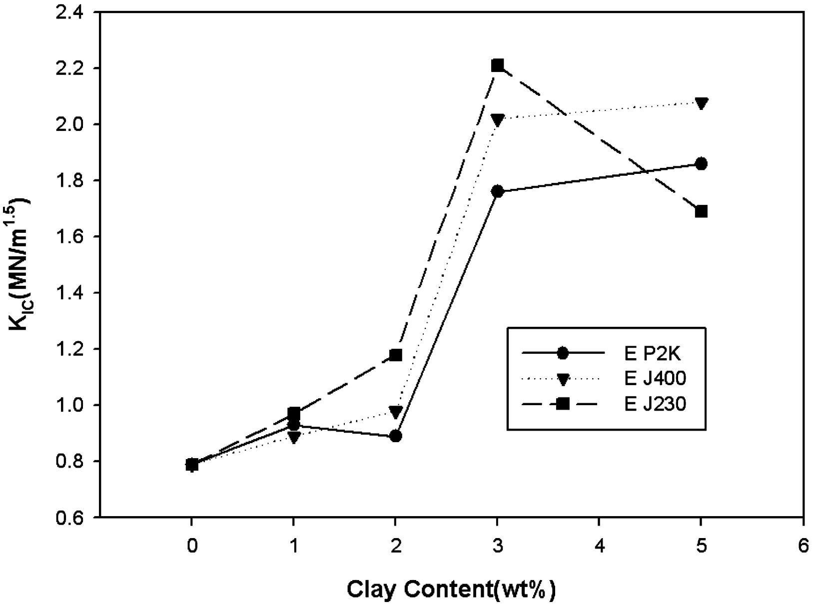

Fig. 12. Critical stress intensity factor(K_{IC}) of epoxy and epoxy/layered silicate nanocomposites.

was 2.78 times higher than that of the neat epoxy specimen. There was not much enhancement when the clay content was varied from 3 to 5%. The epoxy/clay nanocomposites with amine terminated organifier, E J230 and E J400 showed better enhancement when compared to the hydroxyl terminated organifier E P2K and this is related to the higher reactivity of the terminal amine group to epoxy ring compared to the hydroxyl group and the epoxy-silicate interaction is stronger in E J230, E J400 nanocomposites. From our morphology studies, considering the fracture absorbance, aggregated bundles of layer silicates showed better fracture toughness.

4 Conclusions

In this study, reactive organifiers with hydroxyl end-group or amine end-group were synthesized and the morphology, thermal stability, tensile properties and fracture toughness of the epoxy/clay nanocomposites were investigated. The d-spacing of organoclays were found to be 1.98 nm(OC P2K), 1.74 nm (OC J400) and 1.37 nm (OC J230) compared to 1.18 nm of Cloisite®Na^+. The epoxy/layered silicate nanocomposites formed the intercalated structure with some disorder and their d-spacing ranged from 0.9 nm to 5.5 nm. The thermal stability, tensile properties, and fracture toughness significantly increased with increasing the clay content. Comparing the epoxy/clay nanocomposites with organoclays having hydroxyl terminal groups (E P2K series) and the amine terminal groups (E J230 and E J400 series), the nanocomposites with amine terminated organoclay showed higher Young's modulus, tensile strength and fracture toughness due to the stronger interaction between the silicate layer and the epoxy matrix caused by the higher reactivity between the amine end group and the epoxy ring during the curing reaction. Particularly E J230_3 showed the best properties. The modulus increase was 40%, the tensile strength increase was 106% and the fracture toughness increase was 178% when compared to the neat epoxy resin.

References

1. Lan, T., Pinnavaia, T.J., Wang Z.H., Shi and Kavitrana P.D. (1995) *ACS Polym. Mat. Sci. Eng. Proc.*, 73, 250–261.
2. Kelly, P., Akelah, A., Qutubuddin, S. and Moet, A. (1994) *J. Mater. Sci.*, 29, 2274–2280.
3. Messersmith, P.B. and Giannelis, E.P. (1994) *Chem. Mat. Sci.*, 6, 1719–1725.
4. Lan, T., Kaviranta, P.D. and Pinnavaia, T. (1995) *J. Chem. Mater.*, 7, 2144–2150.
5. Philip, G. and Schmidt, H. (1986) *J. Non-Cryst. Solids*, 82, 31–36.
6. Wang, M.S. and Pinnavaia T.J. (1994) *Chem. Mater.*, 6, 2216–2219.
7. Wang, Z. and Pinnavaia, T.J. (1998) *Chem. Mater.*, 10, 1820–1826.
8. Kornmann, X. *Lulea Tekniska Universitet* (2000) p. 12–25.
9. Park, J.H. and Jana, S.C. (2003) *Macromoleules*, 36, 2758–2768.
10. Choi, W.J., Kim, S.H. and Kim, S.C. (2004) *Polymer*, 45, 6045–6057.
11. Hepburn, C. (1992) Polyurethane Elastomers, 2nd ed. Elesevier Science Publishers: Essex, Chapt. 11, 280–282.
12. Usuki, A., Kawasumi, M., Kojima, Y., Okada, A., Kureauchi, T. and Kamigaito, O. (1993) *J. of Mat. Res.*, 8(5), 1174–1178.
13. Eskin, G.I. (2001) *Ultrason. Sonochem.*, 8, 319–325.
14. Chowdhury, F.H., Hosur, M.V. and Jeelani, S. (2006) *Mat. Sci. Eng.*, A421, 298–306.
15. Lam, C., Lau, K., Cheung, H. and Ling, H. (2005) *Mater. Lett.*, 59, 1369–1372.
16. Miyagawa, H., Drzal, L.T. and Carsello, J.A. (2006) *Polym. Eng. Sci.*, 46, 452–463.
17. Vaia, R.A. and Giannelis, E.P. (1997) *Macromolecules*, 30, 8000–8009.
18. Wang, D., Zhu, J., Yao, Q. and Wilkie, C.A. (2002) *Chemistry of Materials,* 14, 3837–3843.
19. Zanetti, M., Camino, G., Thomann, R. and Mülhaupt, R. (2001) *Polymer*, 42, 4501–4507.
20. Noh, M.H., Jang, L.W. and Lee, D.C. (1999) *J. Appl. Polym. Sci.,* 74, 179–188.
21. Wang, Z. and Pinnavaia, T.J. (1998) *Chem. Mater* 10, 3769–3771.